Polym. Bull. (2011) 67:1633–1648
DOI 10.1007/s00289-011-0555-3

ORIGINAL PAPER

Effect of high content of carbon black on non-isothermal crystallization behavior of poly(ethylene terephthalate)

Zhaohui Jiang · Jian Jin · Changfa Xiao · Xin Li

Received: 24 December 2010 / Revised: 6 June 2011 / Accepted: 15 June 2011 /
Published online: 21 June 2011

Abstract With the aid of co-rotating twin screw extruder, poly(ethylene terephthalate) (PET)/carbon black (CB) masterbatches were fabricated through melt-compounding using a separate feeding and metering technique and their homogeneous dispersion morphologies were confirmed by scanning electron microscopy and transmission electron microscopy. Moreover, the ultimate content of CB in the masterbatches was verified via thermogravimetric analysis method. The non-isothermal crystallization process of pristine PET and PET/CB masterbatch were investigated by differential scanning calorimetry and the different methods such as Jeziorny modified Avrami equation, Ozawa equation, and the method developed by Mo were employed to analyze their non-isothermal crystallization kinetics. The results show that CB particles uniformly dispersed in PET matrix act as heterogeneous nucleating agents, while crystallization activation energy (ΔE) of PET/CB masterbatch is much greater than that of virgin PET according to Kissinger formula, Takhor model, and Augis-Bennett model. Whereas, the results obtained from the above mentioned three methods simultaneously demonstrate the addition of CB greatly increases crystallization temperature and crystallinity and accelerates crystallization rate. The results reveal that crystal growth has little effect on the crystallization rate and crystal nucleation dominates the crystallization process of PET/CB masterbatch containing very high CB loading (20 wt%).

Keywords Poly(ethylene terephthalate) · Carbon black · Masterbatch · Nonisothermal · Kinetics

Z. Jiang · C. Xiao
Key Laboratory of Fiber Modification and Functional Fiber,
Tianjin Polytechnic University, Tianjin 300160, China

Z. Jiang · J. Jin (✉) · X. Li
State Key Laboratory of Biobased Fiber Manufacture Technology,
China Textile Academy, Beijing 100025, China
e-mail: jinjian@cta.com.cn

Introduction

Poly(ethylene terephthalate) (PET) is a semi-crystalline polymer and has been extensively used in synthetic fibers and plastics industry due to its excellent spinnability, mechanical properties, heat, and chemical resistance, etc. Currently, some literatures have reported the crystallization behavior of PET and its copolyester [1–5]. In the study of Xianhui Li et al. [6], PET/carbon black (CB) masterbatch containing 3 wt% CB was prepared and non-isothermal crystallization kinetics of the masterbatch was analyzed. As is known, CB could act as nucleating agent in the process of polymer crystallization, which was confirmed in the study of poly(lactic acid)/CB composite [7], polypropylene/CB composite [8, 9], and polyamide/CB composites [10]. In all the mentioned articles, CB content is less than 3 wt%. However, the crystallization behavior of PET/CB masterbatch with high CB content, used as masterbatch for dyeing spinning solution, has been seldom reported. Fortunately, the crystallization rate of PET is so low that there is enough time to complete drawing during spinning process, based on which high-speed spinning of polyester and spinning-drawing by one step can be achieved. Although a small amount of masterbatch is added in spinning process, it would affect the manufacturing process and product performance. The previous study shows that spinnability is closely related to crystallization properties of the melt [11]. In other words, the wide and short crystallization peak is favorable to spin. In addition, since the manufacturing process of polymer undergoes the temperature variety from melt temperature to room temperature, research on the non-isothermal crystallization of PET/CB blending masterbatch is provided with theoretical and practical significance.

To the best of our knowledge, there has been no report in literature that emphasizes the effect of high CB content (more than 20 wt%) on the non-isothermal crystallization behavior of polymer. In this article, masterbatch was prepared by melt blending using a separate feeding technique and differential scanning calorimetry (DSC), an effective technique to evaluate the crystallization process, was employed to investigate the crystallization behavior of PET/CB masterbatch. Emphasis was placed on the heterogeneous nucleation effect of CB particles. Given consideration of crystallization activation energy (ΔE) enhanced and crystallization ability improved, a conclusion that crystal growth has little effect on the crystallization rate and crystal nucleation dominate the crystallization process of PET/CB masterbatch could be drawn.

Experimental

Materials and equipments

PET, semi-delustering, Heng Li Chemical Fiber Co., Ltd., Jiangsu, China, was received in pellet form. CB, N220, primary particle size of 23 nm, was purchased from Tianjin Lihua Jin Chemical Co., Ltd., China. Dispersant (PE wax, $M_w = 4500$–5000 g/mol) was provided by Beijing Chemical Technology University-Rushan joint venture chemical plant.

High speed grinder was purchased from Zhongxing Weiye Co., Ltd., Beijing, China. ZSK-25WLE co-rotate twin-screw extruder, screw diameter (25 mm), L/d (25:1) was made by WP Corporation in Germany. Perkin Elmer Pyris1 DSC, Perkin Elmer, USA, was employed to test the non-isothermal crystallization process of pristine PET and PET/CB masterbatch.

Preparation of PET/CB masterbatch

CB and 0.5 wt% dispersant were first pre-mixed in high speed grinder, and then the dried pellet and CB particles containing a little dispersant were accurately delivered into the twin-screw extruder. The temperature and rotation speed were 270 °C and 200 r/min, respectively. After melt blending, extrusion, cooling, and pelletizing, the cylindrical PET/CB blending masterbatch containing 20 wt% CB was obtained with the size of 2.5 mm (diameter) × 3.5 mm (length).

Scanning electron microscopy (SEM)

For SEM (ISM-6360, Japan) observation, the samples were attached to the sample supports and vacuum coated with a gold layer. The operation was performed at an acceleration voltage of 10 kV. Low and high magnifications were used to consider particles of different level size.

Transmission electron microscopy (TEM)

Samples for TEM analysis were taken randomly from different locations. Ultra thin sections with a thickness of 100 nm were prepared with ultra-sonic diamond knife (Ultrotome 2088, LKB, Sweden). The TEM investigations were performed on a H-800 (HITACHI, Japan) microscope, which was adjusted with an acceleration voltage of 200 kV.

Thermogravimetric analysis (TGA)

The TGA analysis of films was performed on Thermo Gravimetric Analyzer (Pyris1, Perkin Elmer America). The heating process went ahead under the protection of nitrogen atmosphere. The operation was carried out with a heating rate of 20 °C/min in a temperature interval 50–650 °C and kept 650 °C for 5 min.

DSC measurement

The DSC scans of all the samples have been taken at different cooling rates using Perkin Elmer Pyris1 DSC. The temperature precision of the instrument is 0.5 °C. Before the test, the samples were cut into very small pieces and enclosed in aluminum plate. In order to avoid the difference of heat conduction between the samples and stove caused by different weight of samples, the weight of each sample is controlled at the level of about 5 mg. The samples were taken in standard aluminum pans and were heated over a temperature range from room temperature to

290 °C at the heating rates 80 °C/min and hold for 10 min to eliminate thermal history, then cooled to room temperature at the cooling rate 5, 10, 20, and 80 °C/min. All the measurements were carried out under a nitrogen atmosphere.

Results and discussion

Observation of CB dispersion in PET matrix

Figure 1 displays SEM and TEM images of PET/CB masterbatch. As shown in the images, CB particles are well dispersed and uniformly distributed in PET matrix, like the islands in the sea without connection. From images at low magnification, we can estimate that the mean size of CB particles is much less than 1 μm, which we are desired. Besides, in PET/CB masterbatch PET forms a continuous phase and CB particles disperse uniformly. Therefore, although the weight of samples (5 mg) used in DSC measurement is extremely little, the results should not differ greatly because of sampling location.

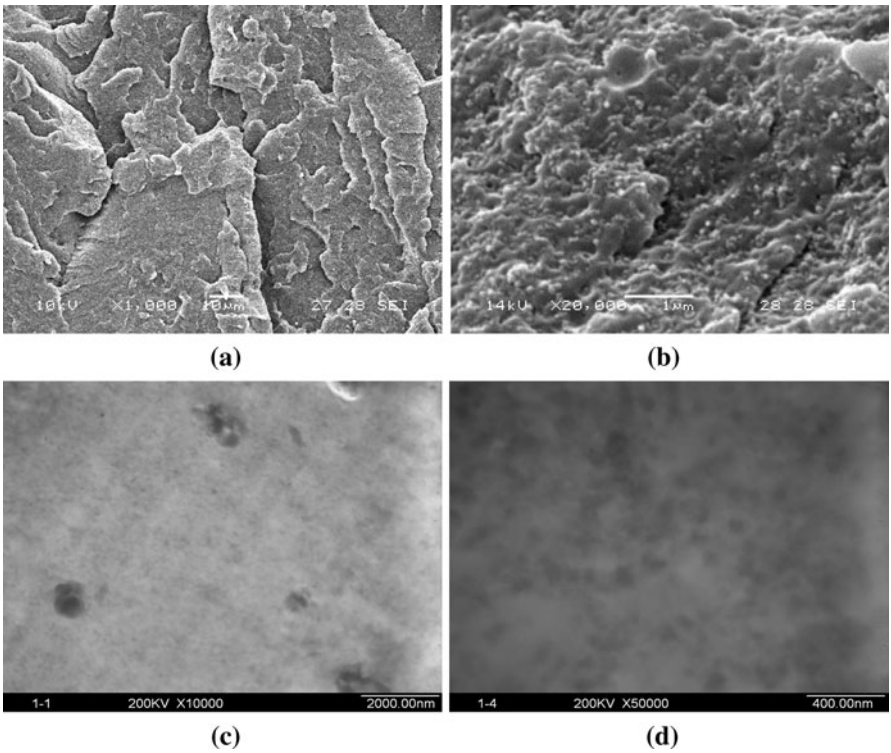

Fig. 1 SEM (**a** 1000×, **b** 20000×) and TEM (**c** 10000×, **d** 20000×) images of PET/CB masterbatch

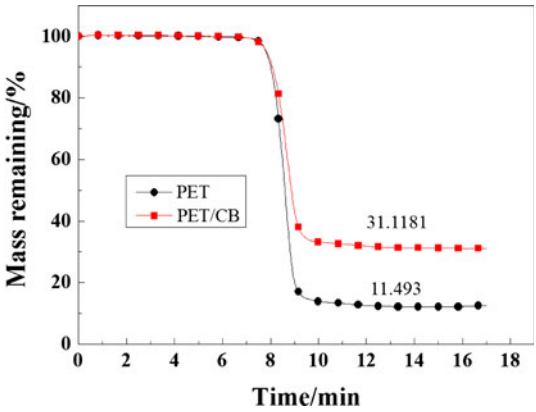

Fig. 2 TGA results for pristine PET and PET/CB masterbatch

TGA results

The ultimate content of CB in PET/CB masterbatch was determined by TGA. The weight loss curves for PET and PET/CB masterbatch are presented in Fig. 2. Analysis of the curves demonstrates that the weight fraction of CB in PET/CB masterbatch is 19.63 wt%, which is very close to the theoretical addition of CB (20 wt%). Simultaneously, this is an indirect evidence of CB particles homogeneously dispersed in PET matrix.

Non-isothermal crystallization characteristics

Based on dynamic crystallization experiment, data for the crystallization exotherms as a function of temperature can be obtained, at the cooling rate of 5, 10, 20, and 80 °C/min, as one can see in Fig. 3 for the crystallization on cooling of PET and PET/CB masterbatch. The crystallization exotherms becomes broader and it shifts to lower temperature with increasing cooling rate. At the same cooling rate, the

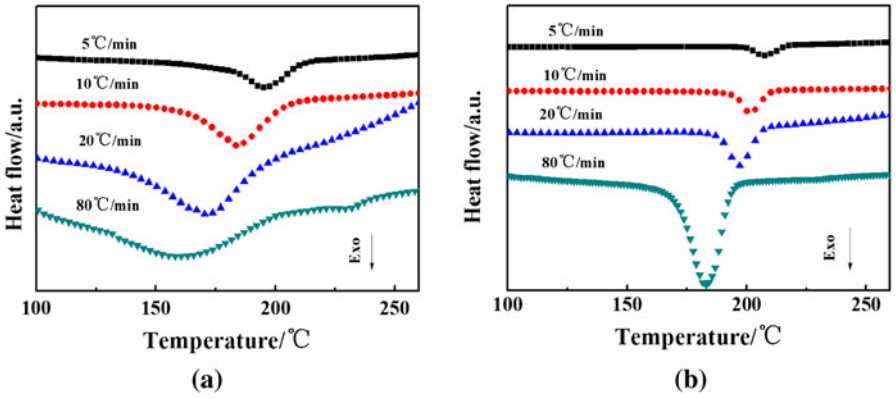

Fig. 3 DSC thermograms of non-isothermal crystallization for PET (**a**) and PET/CB (**b**) masterbatch at various cooling rates

Table 1 Characteristic data of non-isothermal crystallization of PET and PET/CB masterbatch

Samples	Cooling rates (°C/min)	$T_{0.01}$ (°C)	$T_{0.99}$ (°C)	$T_{0.01}$–$T_{0.99}$ (°C)	T_p (°C)	ΔH (J/g)	X_c%
PET	5	212.8	130.6	82.2	194.8	56.6	41.7
	10	209.1	125.5	83.6	184.2	43.3	31.9
	20	207.6	114.4	93.2	170.8	43.1	31.7
	80	201.0	112.6	88.4	160.7	9.2	6.8
PET/CB	5	216.5	196.3	20.1	207.4	47.9	41.1
	10	212.0	180.2	31.9	201.6	38.1	32.6
	20	209.4	170.7	38.7	196.7	45.2	38.7
	80	200.4	145.1	45.2	183.0	30.7	26.3

exotherm peak temperature of PET/CB masterbatch is greater than that of PET. Values of some characteristic parameters, such as the exotherm peak temperature (T_p), the crystallization onset temperature ($T_{0.01}$), the crystallization end temperature ($T_{0.99}$), and other crystallization parameters are summarized in Table 1.

In Table 1, X_c refers to actual crystallinity, which can be calculated by [12]:

$$X_c = \frac{\Delta H_c}{\Delta H_c^0 \times V_m} \times 100\%, \tag{1}$$

where ΔH_c is the crystallization enthalpy, ΔH_c^0 refers to enthalpy of 100% crystalline PET, considered as 135.8 J/g [13], and V_m is weight fraction of PET.

All the results indicate that the values of T_p, $T_{0.01}$, and $T_{0.99}$ shift to lower temperature region. When the polymer melt undergoes low cooling rate, molecular chains have enough time to overcome the nucleation barrier and engage in regular order, so crystallization occurs in high temperature region with a narrow temperature range ($T_{0.01}$–$T_{0.99}$ small), so the crystals develop into larger and better ones. While the melt is under high cooling rate conditions, the activity of molecular chain declines significantly in a short period of time, resulting in the blocked crystallization process owing to the ability of arrangement into the lattice behind the variance of temperature. In this case, the polymer requires greater degree of supercooling and wider temperature range ($T_{0.01}$–$T_{0.99}$ greater) to achieve crystallization balance. Hence, exotherm peak shifts to lower temperature and it could inevitably lead to deteriorated crystallization and relatively lower crystallinity. Furthermore, the exotherm peak temperature and crystallinity of PET/CB masterbatch are higher than that of virgin PET, which implies that act as nucleating agent during the crystallization of the PET matrix. Besides, as the cooling rate increases, the stronger nucleating effect is reflected.

From the data for the crystallization exotherms as a function of temperature dH_c/dT the relative crystallinity as a function of temperature X_t can be formulated as:

$$X_t = \int_{T_0}^{T} (dH_c/dT)dT / \int_{T_0}^{T_\infty} (dH_c/dT)dT, \tag{2}$$

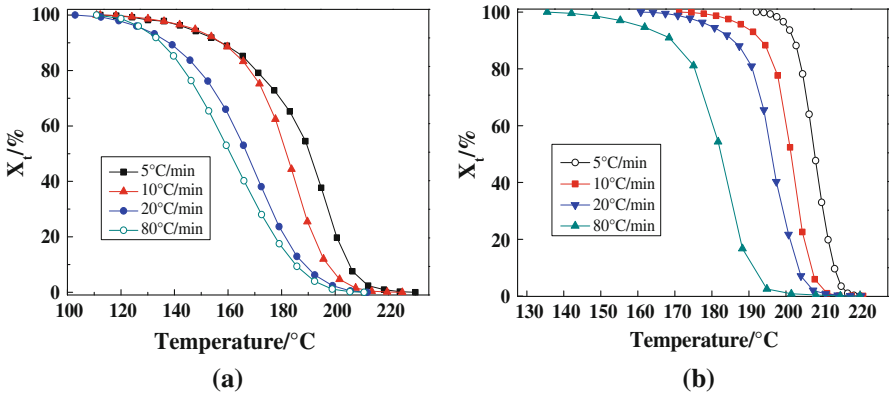

Fig. 4 Plots of X_t versus T at different cooling rates. **a** PET. **b** PET/CB

where T_0 denotes the onset temperature of crystallization and T and T_∞ the crystallization temperature at time t and after the completion of crystallization process, respectively. The evolution of the relative crystallinity as a function of temperature at all different cooling rates appears in Fig. 4. When X_t ranges from 0.2 to 0.8, significant changes in crystallinity occurs.

Crystallization activation energy

To account for the reason of the essential effect of CB particles on the nonisothermal crystallization process of PET and PET/CB masterbatch, several mathematic models were introduced to estimate the crystallization activation energy (ΔE) for the transport of polymer chains toward the growing surface [5]. Considering the variation of peak temperature (T_p) with cooling rate, the activation energy (ΔE) could be determined using the following models:
Kissinger equation [14]:

$$\frac{d[\ln(\varphi/T_p^2)]}{d(1/T_p)} = -\frac{\Delta E}{R} \tag{3}$$

Takhor model [15]:

$$\frac{d[\ln(\varphi)]}{d(1/T_p)} = -\frac{\Delta E}{R} \tag{4}$$

Augis-Bennett model [16]:

$$\frac{d[\ln(\varphi/(T_{0.01} - T_p)]}{d(1/T_p)} = -\frac{\Delta E}{R}, \tag{5}$$

where φ is cooling rate, T_p is exotherm peak temperature, R is the universal gas constant, and ΔE is crystallization activation energy.

Table 2 Crystallization activation energy ΔE (kJ/mol) calculated from Kissinger, Takhor, and Augis-Bennett models

Samples	Kissinger	Takhor	Augis-Bennett
PET	138.2	130.8	127.0
PET/CB	214.0	205.9	203.7

The crystallization activation energy (see Table 2) of PET and PET/CB masterbatch can be obtained from the slope of curve shown in Fig. 5, that is $\Delta E = -R \times$ slope, and the results are listed in Table 2. It states that the activation energy of PET/CB masterbatch is greater than that of virgin PET when anyone of the three models is used. The similar results have been reported by Ge [5] and Achilias et al. [17]. In fact, the addition of CB has the following two effects: on one hand, CB particles play the role of nucleating agent and improve the crystallization ability of PET, which are favorable to PET crystallization. On the other hand, the presence of CB would affect the movement of molecular chains, hinder their access

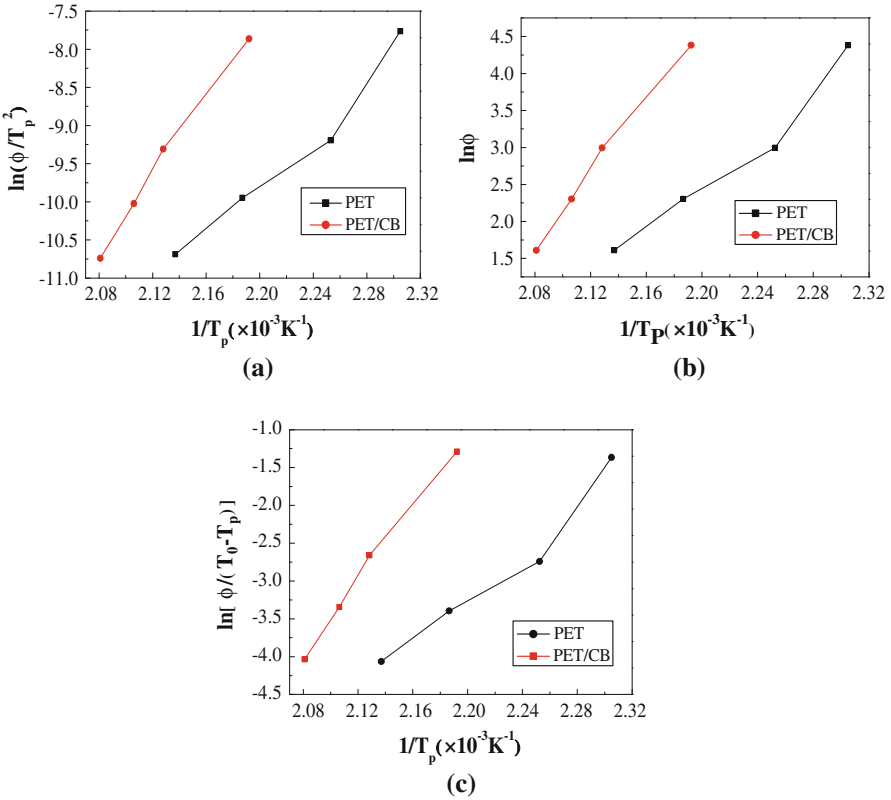

Fig. 5 Plots for estimating the activation energy for nonisothermal of PET and PET/CB masterbatch: **a** Kissinger equation, **b** Takhor model, and **c** Augis-Bennett model

to the lattice and depress the crystallization ability of PET, which are not conducive to PET crystallization. This is a pair of contradictory factors and the final crystallinity is the competition result of the two factors. The data of Fig. 3 and Table 1 imply that CB particles play a positive effect on PET crystallization. Although, CB particles act as nucleating agent in some way, the crystal growth is hindered because the movement molecular chain is significantly hampered. The comprehensive effect of CB in PET crystallization makes crystallization activation energy (ΔE) greatly increase. In Table 1, exotherm peak temperature and crystallinity are enhanced and half crystallization time ($t_{1/2}$) is shortened. This may be due to enough crystal nucleuses because of high CB content and instant formation of numerous small crystals. The conclusion could be drawn that crystal growth has little effect on the crystallization rate and crystal nucleation dominates the crystallization process of PET/CB masterbatch with very high CB content. For furthermore understanding, the non-isothermal crystallization kinetics of PET and PET/CB masterbatch are to be deeply investigated.

Non-isothermal crystallization kinetics

For the analysis of the experimental results of PET and PET/CB masterbatch, the modified Avrami equation, the Ozawa analysis, and the method developed by Mo et al. are tested [18].

Modified Avrami equation

According to the modified Avrami equation, the relative crystallinity (X_t) can be determined by:

$$X_t = 1 - \exp(-Z_t t^n) = 1 - \exp[-(K_{\text{Avramit}})^2], \tag{6}$$

where Z_t and n denote the overall crystallization rate constant and the Avrami exponent, respectively.

Equation 6 can be converted to Eq. 7 as follows:

$$\ln\,[-\ln(1 - X_t)] = \ln\, Z_t + n\ln\, t. \tag{7}$$

Since the rate of non-isothermal crystallization depends on the cooling rate, the following correction has been proposed to obtain the corresponding rate constant at unit cooling rate, Z_c:

$$\ln\, Z_c = \ln\, Z_t/R. \tag{8}$$

Avrami equation is function of the relative crystallinity (X_t) and time (t), so the transformation of temperature (T) and time (t) should be conducted by:

$$t = (T_0 - T)/R \tag{9}$$

where T is the temperature at the time t, T_0 is the onset temperature of crystallization and R is cooling rate.

The point deviating from baseline in Fig. 3 was taken as the origin time [19]. The evolution of relative crystallinity as a function of crystallization time is shown in

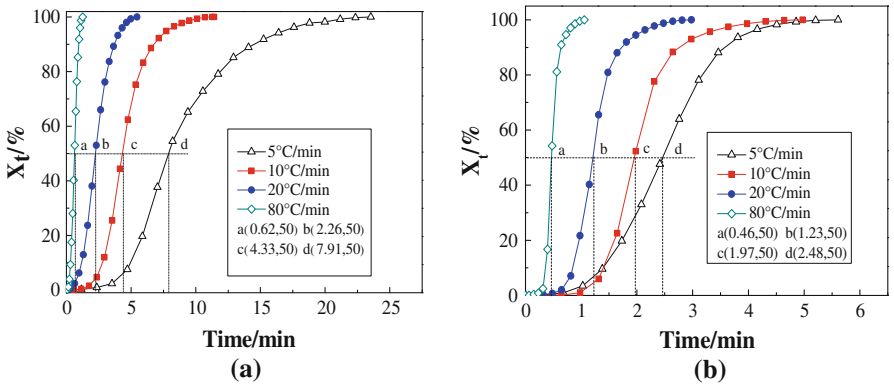

Fig. 6 Evolution of relative crystallinity as a function of crystallization time for PET and PET/CB masterbatch. **a** PET. **b** PET/CB

Fig. 6. S-shaped curves are obtained, which are consistent with nucleation and growth processes. Form these curves, the half time of crystallization, $t_{1/2}$ can be directly determined as the time elapsed from the onset of crystallization to the point where the crystallization is half completed.

There exists a period of crystallization induction time (t_{inc}), which can represent the time in which the polymer is still molten before crystallization. The t_{inc} is defined as:

$$t_{inc} = (T_p - T_{onset})/R. \tag{10}$$

In this article, T_p and T_{onset} can be considered as 290 °C and $T_{0.01}$, respectively. t_{inc} is the time required from melt to nuclei formation, which can reflect the difficulty of nuclei formation. The apparent crystallization time (t_c) can be calculated by:

$$t_c = t_{0.99} - t_{0.01} \tag{11}$$

where t_c is the required time in which apparent crystallization process occurs. $t_{0.01}$ and $t_{0.99}$ are the time when X_t reaches 1 and 99%, respectively. When polymer crystallizes from molten state, the required time $t_{overall}$ is decided by t_{inc} and t_c.

$$t_{overall} = t_{inc} + t_c. \tag{12}$$

According to the previous report [20], $t_{1/2}$ can be deduced as follows:

$$t_{1/2} = [(\ln 2)/Z_t]^{1/n}. \tag{13}$$

The relational parameters for time are listed in Table 3. As it is expected, with increasing cooling rate all the aforementioned characteristic times decrease, which means that the higher the cooling rate the later the crystallization process starts and is completed. Besides, the crystallization time of PET/CB masterbatch is shorter than that of virgin PET. The uniformity of measured and calculated value of $t_{1/2}$ states clearly that modified Avrami equation can be used to describe the non-isothermal crystallization kinetics of PET and PET/CB masterbatch.

Table 3 The time parameters for virgin PET and PET/CB masterbatch in process of crystallization

Samples	Cooling rates (°C/min)	$t_{0.01}$ (min)	$t_{0.99}$ (min)	$t_{1/2}$ (min) (measured)	$t_{1/2}$ (min) (calculated)	t_c (min)	t_{inc} (min)	$t_{overall}$ (min)
PET	5	2.6	21.8	7.9	10.5	19.2	15.4	34.6
	10	1.4	9.9	4.3	5.0	8.5	8.1	16.6
	20	1.2	4.8	2.3	2.3	3.6	4.1	7.7
	80	0.2	1.2	0.6	0.6	1.0	1.1	2.1
PET/CB	5	0.8	4.9	2.5	2.5	4.1	14.7	18.8
	10	1.0	4.5	2.0	2.3	3.5	8.0	11.5
	20	0.6	2.6	1.2	1.4	2.0	4.2	6.2
	80	0.3	0.9	0.5	0.5	0.7	1.2	1.9

The relationships between $\ln[-\ln(1 - X_t)]$ and $\ln t$ for PET and PET/CB masterbatch are illustrated in Fig. 7. For PET and PET/CB masterbatch at any cooling rate, the curves in whole crystallization process are not strictly linear, but the main crystallization process (initial stage) follows Avrami equation. At the later stage, the curves deviate from the linear relationship because of secondary crystallization and spherulite impingement [6, 7]. Besides, the addition of CB increases the viscosity of the system and the movement of molecular chains is restricted, so it must take a long time for the system from completely disordered state to three-dimensional ordered crystals. The delayed crystallization will occur for some molecular chains. Therefore, the deviation in curves of PET/CB masterbatch is greater than that of PET. Similar results were also observed in PET/clay [21], isotactic PP/CB [22].

Based on Eq. 9, a linear curve fitting procedure is employed. From the slope and intercept of the straight line, n and $\ln Z_t$ can be obtained, respectively. The fitting values for the parameters are presented in Table 4. It is obvious that the modified Avrami method can describe the experimental data very well at initial stage. Although physical meaning of n and Z_t cannot be related to the non-isothermal case

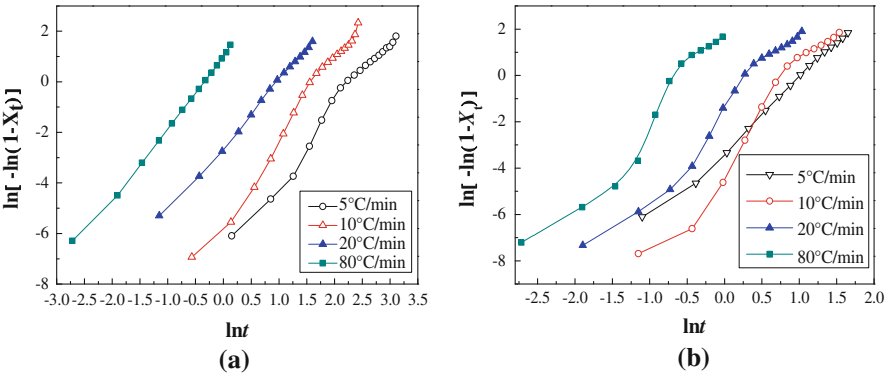

Fig. 7 Plots of $\ln[-\ln(1 - X_t)]$ versus $\ln t$. **a** PET. **b** PET/CB

Table 4 Results of the Avrami analysis for non-isothermal crystallization of PET and PET/CB masterbatch

Samples	Cooling rates (°C/min)	n	ln Z_t	Z_t	ln Z_c	Z_c
PET	5	2.778	−6.618	0.001	−1.324	0.266
	10	3.205	−5.470	0.004	−0.547	0.579
	20	2.563	−2.527	0.080	−0.126	0.881
	80	2.766	0.962	2.612	0.012	1.012
PET/CB	5	3.045	−3.152	0.043	−0.630	0.533
	10	3.995	−3.733	0.024	−0.373	0.689
	20	3.526	−1.485	0.226	−0.074	0.929
	80	3.794	1.974	7.200	0.025	1.025

in a simple way, their use provides further insight into the kinetics of non-isothermal crystallization. The values of n for virgin PET are around 3.0, indicating that the crystal growth is three-dimensional (spherulitic) with homogeneous nucleation, which agrees with the results observed by Li [6] and Wan [21]. The n of PET/CB masterbatch ranges from 3 to 4, greater than that of virgin PET, which indicates that the mechanisms of the non-isothermal crystallization of PET/CB masterbatch is more complicated than that of virgin PET. Similar results were also observed in PET/disodium terephthalate (DST) [23] and PET/silica [24] in isothermal crystallization. Obviously, CB works on the mechanism of nucleation and crystal growth of PET [23–25]. Furthermore, according to the mode of evolution of PET spherulite revealed by Lee, Bian proposed that n values are related to the number of growth points in crystallization process, the greater n values, the more growth points. Hence, for PET/CB masterbatch, the increasing of growth points leads to the greater n values. The crystallization constant, Z_t, increases with increasing cooling rate attributed to supercooling. In addition, Z_t and Z_c of PET/CB masterbatch are greater than those of PET, which implies that the crystallization rate of PET/CB masterbatch is faster than that of PET, in agreement with the results of $t_{1/2}$.

Ozawa analysis

As we all know, the Avrami equation for a non-isothermal crystallization process may be considered as just the same mode for an isothermal crystallization process, but it does not take into account the factors that are special for non-isothermal processes, such as cooling rate and the temperature variation at different time [7]. According to the Ozawa theory, the non-isothermal crystallization process is the result of an infinite number of small isothermal crystallization steps and the degree of conversion at temperature T, X_t can be written as a function of cooling rate (R) as follows:

$$1 - X_t = \exp(-K/R^m), \tag{14}$$

where K is the cooling or heating crystallization function, which is related to the

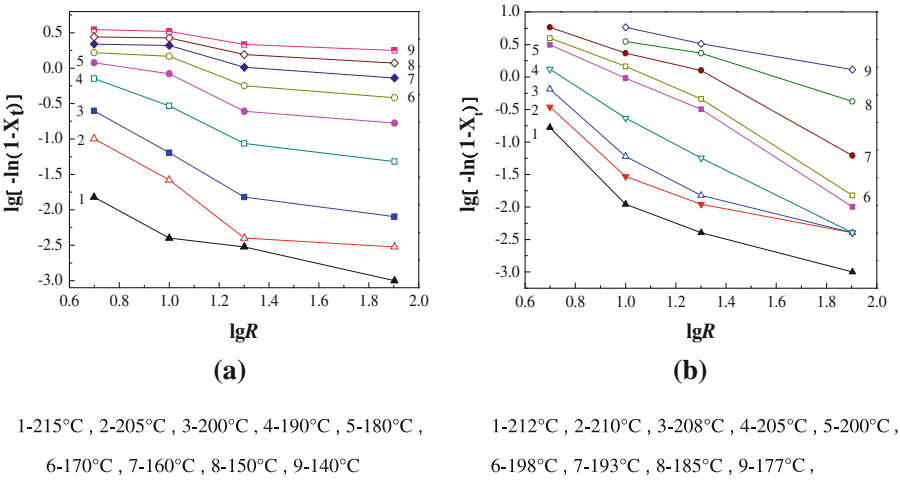

Fig. 8 Plots of lg[−ln(1 −X_t)] versus lg$R$. **a** PET. **b** PET/CB

overall crystallization rate and indicates how fast crystallization occurs. m is the Ozawa exponent that depends on the dimension of crystal growth. Taking the double-logarithmic form of Eq. 14, it follows:

$$\lg[-\ln(1 - X_t)] = \lg K - m \lg R \tag{15}$$

By plotting lg[−ln(1 − X_t)] versus lg R, a straight line should be obtained and the kinetic parameters, K and m can be achieved from the slope and the intercept, respectively. Indicative Ozawa plots for crystallization of PET and PET/CB masterbatch are illustrated in Fig. 8. For virgin PET, none of good straight lines were obtained in broad temperature range, declaring the Ozawa model does not works well. However, the Ozawa equation can describe the process of non-isothermal crystallization of PET/CB masterbatch satisfactorily during the temperature range of 205–177 °C. Throughout the crystallization process, the curves do not show a good linear relationship, which indicates that n is not a constant. Thus, the Ozawa method can not fully describe the non-isothermal crystallization process of PET and PET/CB masterbatch.

Mo's method

Non-isothermal crystallization is difficult to describe with a single equation since there are a lot of parameters that have to be taken into account simultaneously. The importance of this method is that it correlates the cooling rate to temperature, time, and morphology. Mo et al. [26] proposed a novel kinetic method by combining the Ozawa and Avrami equations. As the degree of crystallinity was related to the cooling rate, R, and the crystallization time t and temperature T, the relation between R and t could be defined for a given degree of crystallinity. Consequently, combining Eqs. 7 and 15 derived a new kinetic model for non-isothermal crystallization:

$$\ln Z_t + n\ln t = \ln K(T) - m\ln R. \tag{16}$$

After rearrangement at a given crystallinity, Eq. 16 is transferred into the following form:

$$\ln R = \ln F(T) - a\ln t, \tag{17}$$

where $F(T) = [K(T)/Z_t]^{1/m}$ refers to the value of the cooling rate chosen at unit crystallization time, when the system has a certain degree of crystallinity. a is the ratio of the Avrami exponent n to the Ozawa exponent m ($a = n/m$). According to Eq. 17, at a given degree of crystallinity the plot of ln R against ln t will give a straight line with an intercept of ln $F(T)$ and a slope of −a. As it is shown in Fig. 9, plotting ln R versus ln t, at a given degree of crystallinity, a linear relationship is observed. The values of $F(T)$ and the slope a are summarized in Table 5. The value of a is almost a constant, while $F(T)$ increases with the increasing of relative crystallinity for both PET and PET/CB masterbatch. This states clearly that higher cooling rate is required to obtain a higher degree of relative crystallinity. When relative crystallinity is equipotent, the $F(T)$ of PET is greater than that of PET/CB masterbatch, which reveals that CB affects the mechanism of nucleation and crystal growth of PET and accelerates the crystallization rate of PET, in agreement of results of Avrami equation. Obviously, comparing with Ozawa and Avrami

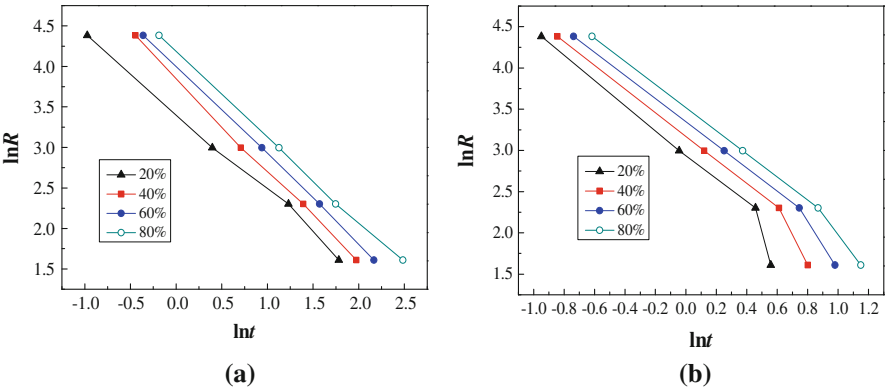

Fig. 9 Plots of ln R versus ln t. **a** PET. **b** PET/CB

Table 5 Values of a and $F(T)$ versus degree of crystallinity based on Mo's method

Samples	X_t (%)	a	ln $F(T)$	$F(T)$
PET	20	0.986	3.423	30.661
	40	1.138	3.856	47.276
	60	1.093	4.002	54.707
	80	1.046	4.174	64.975
PET/CB	20	1.688	2.832	16.980
	40	1.591	3.097	22.131
	60	1.542	3.300	27.113
	80	1.518	3.496	32.983

equation, Mo's method can describe the non-isothermal crystallization of PET and PET/CB masterbatch more successfully.

Conclusions

CB particles in PET/CB masterbatch were uniformly dispersed conformed by SEM and TEM. Besides, the ultimate content of CB was verified via TGA method.

The CB particles dispersed in PET matrix act as heterogeneous nucleating agents, so it increases crystallization temperature and crystallinity and accelerates crystallization rate. Although, CB particles play a role as heterogeneous nucleating agents, high CB content hinders the movement of PET molecular chains. The combined result of both roles of CB shows that the addition of CB increases the crystallization ability of PET. Furthermore, the different methods such as Jeziorny modified Avrami equation, Ozawa equation, and the method developed by Mo are employed to analyze the non-isothermal kinetics of virgin PET and PET/CB masterbatch, in which Mo method is proven to be a suitable one for the study, they all confirm that CB particles promote PET crystallization. Besides, the crystallization activation energy (ΔE) of PET/CB masterbatch is much greater than that of virgin PET according to Kissinger formula, Takhor model, and Augis-Bennett model, which demonstrates that crystal growth has little effect on the crystallization rate and crystal nucleation dominate the crystallization process of PET/CB masterbatch with very high CB content.

Acknowledgments The authors gratefully acknowledge the financial support of the National Science and Technology Supporting Item (2009BAE75B01).

References

1. Verhpyen O, Dupret F, Legras R (1999) Isothermal and non-isothermal crystallization kinetics of polyethylene terephthalate: mathematical modeling and experimental measurement. Polym Eng Sci 38:1594–1610
2. Anand KA, Agarwal US, Joseph R (2006) Carbon nanotubes induced crystallization of poly(ethylene terephthalate). Polymer 47:3976–3980
3. Cai D, Zhang Y, Chen YM (2007) Effect of organic modification of SiO_2 on non-isothermal crystallization of PET in PET/SiO_2 nanocomposites. Iran Polym J 16:851–859
4. Xanthos M, Baltzis BC, Hsu PP (1997) Effects of carbonate salts on crystallization kinetics and properties of recycled poly(ethylene terephthalate). J Appl Polym Sci 64:1423–1435
5. Ge CH, Shi LY, Yang H, Tang SF (2010) Nonisothermal melt crystallization kinetics of poly(ethylene terephthalate)/barite nanocomposites. Polym Compos 31:1504–1514
6. Li XH, Guo WH, Zhou QL, Xu SA, Wu CF (2007) Non-isothermal crystallization kinetics of poly (ethylene terephthalate)/grafted carbon black composite. Polym Bull 59:685–697
7. Su ZZ, Guo WH, Liu YJ, Li QY, Wu CF (2009) Non-isothermal crystallization kinetics of poly(lactic acid)/modified carbon black composite. Polym Bull 62:629–642
8. Mucha M, Krolikowski Z (2003) Application of DSC to study crystallization kinetics of polypropylene containing fillers. J Therm Anal Calorim 74:549–557
9. Wiemann K, Kaminsky W, Gojny FH, Schulte K (2005) Synthesis and properties of syndiotactic poly(propylene)/carbon nanofiber and nanotube composites prepared by in situ polymerization with metallocene/MAO catalysts. Macromol Chem Phys 206:1472–1478

10. Del RC, Ojeda MC, Acosta JL (2000) Carbon black effect on the microstructure of incompatible polymer blends. Eur Polym J 36:1687–1695
11. Zheng H, Wu JL (2007) Preparation, crystallization, and spinnability of poly(ethylene terephthalate)/silica nanocomposites. J Appl Polym Sci 103:2564–2568
12. Jiang ZH, Xiao CF, Wang X, Hu XY (2010) Structure and performance of polyamide-6 membranes prepared by thermally induced phase separation. Chin J Polym Sci 28:721–729
13. Dong W, Zhao J, Li CX, Guo ML, Zhao DL, Fan QR (2002) Study of the amorphous phase in semicrystalline poly(ethylene terephthalate) via dynamic mechanical thermal analysis. Polym Bull 49:197–203
14. Huang JW, Huang YC, Wen YL, Kang CC, Yeh MY (2009) Polylactide/nano- and micro-scale silica composite films. II. Melting behavior and cold crystallization. J Appl Polym Sci 112:3149–3156
15. Wu M, Yang GZ, Wang M, Wang WZ, Zhang WD, Feng JC, Liu TX (2008) Nonisothermal crystallization kinetics of ZnO nanorod filled polyamide 11 composites. Mater Chem Phys 109:547–555
16. Yang GZ, Chen XL, Wang WZ, Wang M, Liu TX, Li CZ (2007) Nonisothermal crystallization and melting behavior of a luminescent conjugated polymer, poly(9, 9-dihexylfluorene-alt-co-2, 5-didecyloxy-1, 4-phenylene). J Polym Sci Part B Polym Phys 45:976–987
17. Achilias DS, Bikiaris DN, Papastergiadis E, Giliopoulos D, Papageorgiou GZ (2010) Characterization and crystallization kinetics of in situ prepared poly(propylene terephthalate)/SiO_2 nanocomposites. Macromol Chem Phys 211:66–79
18. Liu XH, Fang JQ, Qi ZN (2001) Study on non-isothermal crystallization kinetics of polypropylene/montmorillonite nanocomposites. Polym Mater Sci Eng 17:103–110
19. Qin ZZ, Wang YY (1999) Study on non-isothermal crystallization behavior of modified PET. China Synth Fiber Ind 22:21–24
20. Xu WB, Ge ML, He PS (2001) Study on non-isothermal crystallization kinetics of polypropylene/montmorillonite nanocomposites. Acta Polym Sin 10:585–588
21. Wang T, Chen L, Chua YC, Lu X (2004) Crystalline morphology and isothermal crystallization kinetics of poly(ethylene terephthalate)/clay nanocomposites. J Appl Polym Sci 94:1381–1388
22. Mucha M, Marszalek J, Fidrych A (2000) Crystallization of isotactic polypropylene containing carbon black as a filler. Polymer 41:4137–4142
23. Bian J, Ye SR, Feng LX (2003) Heterogeneous nucleation on the crystallization poly(ethylene terephthalate). J Polym Sci Part B Polym Phys 41:2135–2144
24. Chae DW, Kim BC (2007) Effects of introducing silica particles on the rheological properties and crystallization behavior of poly(ethylene terephthalate). J Mater Sci 42:1238–1244
25. Kim JY, Park HS, Kim SH (2007) Multiwall-carbon-nanotube-reinforced poly(ethylene terephthalate) nanocomposites by melt compounding. J Appl Polym Sci 103:1450–1457
26. Liu T, Mo Z, Wang S, Zhang H (1997) Nonisothermal melt and cold crystallization kinetics of poly(aryl ether ether ketone ketone). Polym Eng Sci 37:568–575